Spin excitations in the longitudinally modulated magnetic phase of erbium

R. M. Nicklow

Solid State Division, Oak Ridge National Laboratory, Oak Ridge, Tennessee 37831

N. Wakabayashi

Department of Physics, Keio University, Yokohama 223, Tokyo, Japan

(Received 12 December 1994)

The magnetic excitations propagating along the c axis in the longitudinally modulated magnetic phase of erbium metal have been measured as a function of temperature by neutron inelastic scattering. Both transverse and longitudinal excitations have been studied. Some measurements have also been carried out for the paramagnetic phase. The results for the ordered phase are in substantial agreement with calculations based on a random-phase-approximation theory and previously published parameters for the exchange and crystal-field interactions.

I. INTRODUCTION

Erbium is a heavy rare-earth (hcp) metal with a variety of unusual magnetic structures.[1-3] Between 52 K and T_N (~ 85 K), the ordered component of the Er moment is parallel to the c axis and its magnitude varies sinusoidally as one moves along the c direction. In this c-axis amplitude-modulated phase (CAM), the modulation wave vector $\tau = (0,0,\tau_0)2\pi/c$ is not commensurate with the crystal lattice periodicity, although τ_0 is within 2% of ($\frac{2}{7}$). Previous neutron-scattering measurements[4] of the transverse-magnetic excitations in the c direction of this phase showed a rather featureless, broad intensity distribution in energy which showed some dependence on the scattering vector **Q**. While the broad distribution was qualitatively consistent with expectations, the data were not quantitatively analyzed due to a lack of appropriate theoretical models.

Recently, quite different theoretical approaches for calculating the excitations of a longitudinally modulated spin structure have been developed. The theory of Lovesey,[5] and its application to Er by Lantwin,[6] involves an analytic mathematical formulation, based on linear spin-wave theory, for the transverse dynamic susceptibility at $T = 0$ K. The main features of these results include (1) a broad continuum of excitation energies with a finite neutron-scattering cross section at $\hbar\omega = 0$ and (2) several sharp peaks (singularities) at and near the top of the continuum. Both of these features were found to be nearly independent of the excitation wave vector **q**. The theory of McEwen, Steigenberger, and Jensen[7] is a random-phase-approximation (RPA) theory that involves a numerical diagonalization of the molecular-field (MF) Hamiltonian. It explicitly includes magnetoelastic interactions, crystal-field anisotropy, and finite temperatures. However, they have applied it only to thulium.

In view of this recent theoretical work, we have carried out new and more extensive neutron-inelastic-scattering experiments on Er in the CAM phase. The new measurements bear no resemblance to the theoretical results obtained for Er by Lantwin.[6] Therefore, we have carried out our own calculations for Er based on the RPA theory described by McEwen, Steigenberger, and Jensen.[7]

II. THE RPA MODEL FOR Er

The theory is based on the usual magnetic Hamiltonian for the rare-earth metals:[7]

$$\mathcal{H} = \sum_i \left[\sum_{l=2,4,6} B_l^0 O_l^0(\mathbf{J}_i) + B_6^6 O_6^6(\mathbf{J}_i) \right] - \sum_{i>j} J_{i,j} \mathbf{J}_i \cdot \mathbf{J}_j \ . \quad (1)$$

The first two terms represent the single-ion crystal-field interactions expressed as a product of the parameters B_l^m and the Stevens operators O_l^m, while the third term is the Ruderman-Kittel-Kasuya-Yosida exchange interaction. When the excitation wave vector **q** is along the c axis, the Fourier transform of the exchange interaction can be written:

$$J(\mathbf{q}) = J_0 + 2 \sum_{n=1} J_n \cos(n\mathbf{q}c/2) \ , \quad (2)$$

where J_n represents the interplanar coupling constants. J_n is the sum of the exchange interactions between an atom in the "origin" basal plane and all the atoms in a similar plane displaced a distance $nc/2$ along **c**. In our calculations we have neglected dipole-dipole coupling and magnetoelastic interactions. We have assumed also that the spin structure is commensurate with the crystal. In the case of Er, with the modulation wave vector $|\tau|$ so near to $(2/7)(2\pi/c)$, it is reasonable to choose a magnetic unit cell which consists of seven hexagonal layers. Since we are considering **q** only along the c axis, the theory can be developed as if we were treating a one-dimensional (1D) system.

Our calculation follows closely that described by McEwen, Steigenberger, and Jensen.[7] The first step is to determine the MF eigenvalues and eigenvectors for the atoms in each of the seven layers in the magnetic cell.

We begin by assuming a distribution for the moments $\langle \mathbf{J}_k \rangle$ at a given temperature T. For Er, in the temperature range of our measurements, a very good *initial* guess for the distribution of the $\langle \mathbf{J}_k \rangle$ is sinusoidal, i.e., $\langle \mathbf{J}_k \rangle = \langle \mathbf{J} \rangle_{\text{max}} \cos[2\pi(k-1)/7]$. These values are then inserted in the MF Hamiltonian for an atom in the *i*th layer, which is then diagonalized. From the resulting eigenvalues and eigenvectors, the partition function and a new value for $\langle \mathbf{J}_i \rangle$ is calculated. This calculation is carried out for all of the seven layers in the cell and the procedure is repeated until self-consistency is achieved. Obviously, the results obtained depend on the values used for the crystal-field parameters B_l^m and the exchange constants J_n. We have used the J_n $(n>0)$ deduced by Lindgård[8] from an analysis of the low-temperature spin-wave dispersion for Er (Ref. 9) (see Table I) and the B_l^m reported by Høg and Touborg[10] (see set A in Table II). We determined J_0 in this study by requiring the model to reproduce an ordering temperature T_N (defined as the lowest temperature for which all $\langle \mathbf{J}_i \rangle = 0$) that is close to the measured value. The model gives $T_N = 83.4$ K, whereas the value we measured in this experiment is about 87 K. In all of the comparisons between theory and experiment, we have made the comparisons for the same ratio T/T_N. We have not attempted to use our data to determine any of the parameters in the model. However, other sets of parameters for Er have been reported in the literature and we will compare briefly some results obtained with the different sets.

The next step in the calculation is to use the MF eigenvalues and eigenvectors determined as discussed above to calculate the single-site Green function $g(i,\omega)$ for each of the seven sites i by using Eq. (5) of McEwen, Steigenberger, and Jensen.[7] As discussed in this reference, it is necessary to introduce a finite-energy width ϵ for the MF levels of the magnetic system. A value of 0.5 meV was used in the following analysis.

The intensity of the scattered neutrons is determined by the two-site Green function $G_{\alpha\beta}(i,j;\omega)$. Since the magnetic unit cell contains seven nonequivalent moments, the Fourier transform of the two-site Green function leads to seven 3×3 matrices $G_s^{\alpha\beta}(\mathbf{Q},\omega)$, with $(s=0,1,\ldots,6; \alpha,\beta=x,y,z)$. In the RPA theory these are coupled to each other through the equations

$$G_s^{\alpha\beta}(\mathbf{Q},\omega) = g_s^{\alpha\beta}(\omega)$$
$$- \sum_{r=0}^{6} \sum_{\mu\nu} g_s^{\alpha\mu}{}_r(\omega) J_{\mu\nu}(\mathbf{Q}+r\tau) G_r^{\nu\beta}(\mathbf{Q},\omega) , \quad (3)$$

where $g_s^{\alpha\beta}(\omega)$ and $J_{\mu\nu}(\mathbf{Q})$ represent the Fourier transforms of the single-site Green function and the exchange

TABLE I. Interplanar exchange coupling parameters (meV).

n	0	1	2	3	4	5
J_n	0.181	0.053	-0.021	-0.003	-0.012	-0.006

TABLE II. Crystal-field parameters (meV).

Set	B_2^0	B_4^0	B_6^0	B_6^6	Ref.
A	-0.027	0.52×10^{-4}	0.21×10^{-5}	-0.24×10^{-4}	10
B	-0.027	-0.3×10^{-4}	0.13×10^{-5}	-0.09×10^{-4}	3
C	-0.027	-0.07×10^{-4}	0.08×10^{-5}	-0.069×10^{-4}	12

interaction, respectively. McEwen, Steigenberger, and Jensen solved Eq. (3) for $G_s^{\alpha\beta}(\mathbf{Q},\omega)$ by iteration. We obtained G_s by regarding the equation as a matrix equation, instead. If the Green functions g and G are regarded as the elements of 21×3 matrices, the above equations can be written in matrix form as

$$\mathbf{HG} = \mathbf{g} , \quad (4)$$

where $\mathbf{H}$ is a 21×21 matrix with elements defined as

$$H_{\alpha\beta}^{sr} = \delta_{\alpha s,\beta r} + \sum_{\mu} g_s^{\alpha\mu}{}_r(\omega) J_{\mu\beta}(\mathbf{Q}+r\tau) . \quad (5)$$

The two-site Green function is then obtained by solving the matrix equation given in Eq. (4). The neutron scattering intensity is proportional to the scattering function

$$S(\mathbf{Q},\omega) = -\sum_{\alpha\beta} (\delta_{\alpha\beta} - Q_\alpha Q_\beta/Q^2) S_{\alpha\beta}(\mathbf{Q},\omega) , \quad (6)$$

where $S_{\alpha\beta}(\mathbf{Q},\omega)$ is defined as,

$$S_{\alpha\beta}(\mathbf{Q},\omega) = (1 - e^{-\hbar\omega/kT})^{-1} \frac{1}{\pi} \text{Im} G_{s=0}^{\alpha\beta}(\mathbf{Q},\omega) .$$

III. EXPERIMENTAL DETAILS

The measurements were carried out on a crystal of about 1.5 cm^3, enriched (96%) in the low neutron capturing isotope ^{170}Er, that was grown at the Oak Ridge National Laboratory (ORNL). The experiments were performed on the HB2 and HB3 triple-axes spectrometers located at the High Flux Isotope Reactor (HFIR) of ORNL. The monochromator and analyzer were the (002) planes of pyrolytic graphite (PG). The monochromator was vertically focused with the focusing radius under computer control in order to maintain optimum focusing conditions as the neutron energy changed during each scan. All measurements were constant-$\mathbf{Q}$ scans with the scattered neutron energy fixed at 13.7 meV. A PG filter was placed in the scattered beam to reduce possible spurious signals from harmonic wavelength contamination. However, with an unfiltered incident beam, the beam-monitor detector in front of the sample does not measure correctly the intensity of the beam incident on the sample. All the data were corrected for this effect as discussed in a previous publication.[11]

The collimation, in the usual notation, was 40'-20'-20'-30'. This resulted in an energy resolution, full width at

half maximum, ranging from about 0.52 meV (measured with vanadium) for zero energy transfer to 0.75 meV (calculated) for an energy transfer of 5.0 meV.

Measurements were carried out for various temperatures in the 60–200 K range and for several scattering vectors $\mathbf{Q}$ both parallel and perpendicular to the c axis. Since the direction of the ordered moment is along the c axis, scattering by the transverse excitations, i.e., $S_{xx}(\mathbf{Q},\omega)+S_{yy}(\mathbf{Q},\omega)=2S_{xx}(\mathbf{Q},\omega)$, is observed for $\mathbf{Q}\|c$ and $S_{xx}(\mathbf{Q},\omega)+S_{zz}(\mathbf{Q},\omega)$ is observed for the $\mathbf{Q}\|c$ axis. In terms of the usual coordinate system in which the Miller indices (hkl) identify Bragg diffraction positions in the hcp reciprocal space, the measurements reported below correspond to scattering vectors with coordinates $(0,0,2+\zeta)$ and $(1,1,\zeta)$. The primary Bragg diffraction peaks of the *magnetic* structure are observed when $\mathbf{Q}\sim\perp c$ at $\zeta=\tau_0$, e.g., at $(1,1,\tau_0)$. In addition, for the lowest temperatures in the range studied and for $\mathbf{Q}\perp c$, small but significant elastic intensity is observed also at values of $\zeta=3\tau_0$ and $5\tau_0$, corresponding to the locations of the diffraction peaks of the higher-order harmonics of the magnetic structure. To avoid these positions, we have made measurements primarily for values of $\zeta=0.10$, 0.53, 0.62, 0.80, and 0.92 for both $\mathbf{Q}\perp c$ and $\mathbf{Q}\|c$. Note that $\tau_0\approx0.29$.

IV. RESULTS

The results obtained for the transverse excitations at $T=60$ K are shown in Fig. 1. The lines were calculated
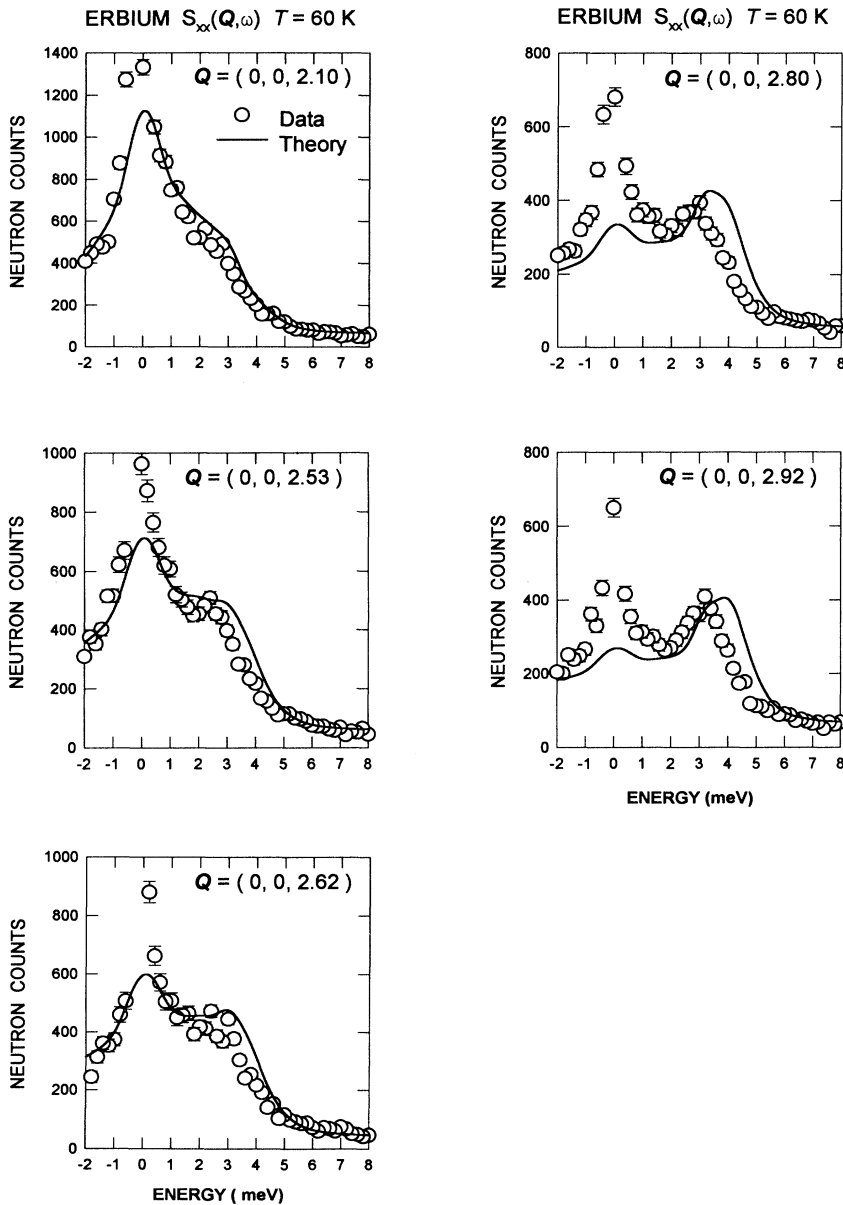

FIG. 1. Calculated and measured intensities for the transverse neutron-scattering function of erbium at 60 K.

from the theory and are proportional to $2S_{xx}(\mathbf{Q},\omega)$. All calculations were "folded" with the resolution function before comparison with the data. The calculations for $\mathbf{Q}=(0,0,2.92)$ were scaled to make the calculated peak intensity in the range 3–4 meV agree approximately with the measurements. The same scale factor was then used for all other comparisons between theory and experiment at other $\mathbf{Q}$ and at the other temperatures discussed below. The theory accounts for most of the observations for energy transfers above about 1.0 meV. The main discrepancy is in the $\mathbf{Q}$ dependence of the "quasielastic" scattering.

The peak in the scattering around 3–4 meV at large $\mathbf{Q}$ can be understood from the calculated energies of the crystal-field levels. The energies of the excited levels relative to that of the ground state obtained from the parameters of Høg and Touborg[10] are plotted in Fig. 2 as a function of the molecular field. From the self-consistent calculation for the $\langle \mathbf{J}_i \rangle$, discussed above, the magnitude of the molecular field experienced by an Er atom at 60 K ranges from 0 to about 2 meV, depending on whether the
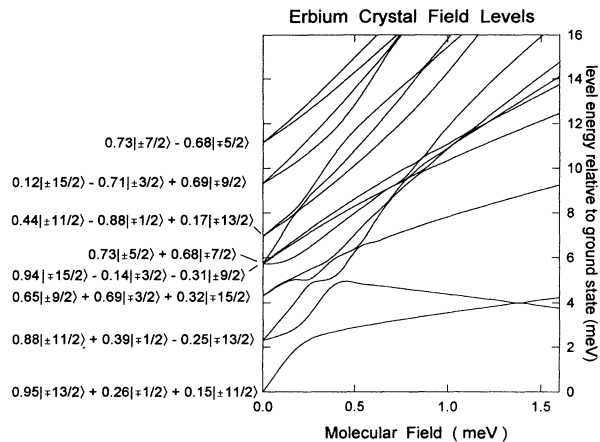

FIG. 2. The crystal-field levels in erbium from the parameters in Table II, set A, as a function of the molecular field. The energy plotted is relative to the ground state. The state vectors to the left are the zero-field states.
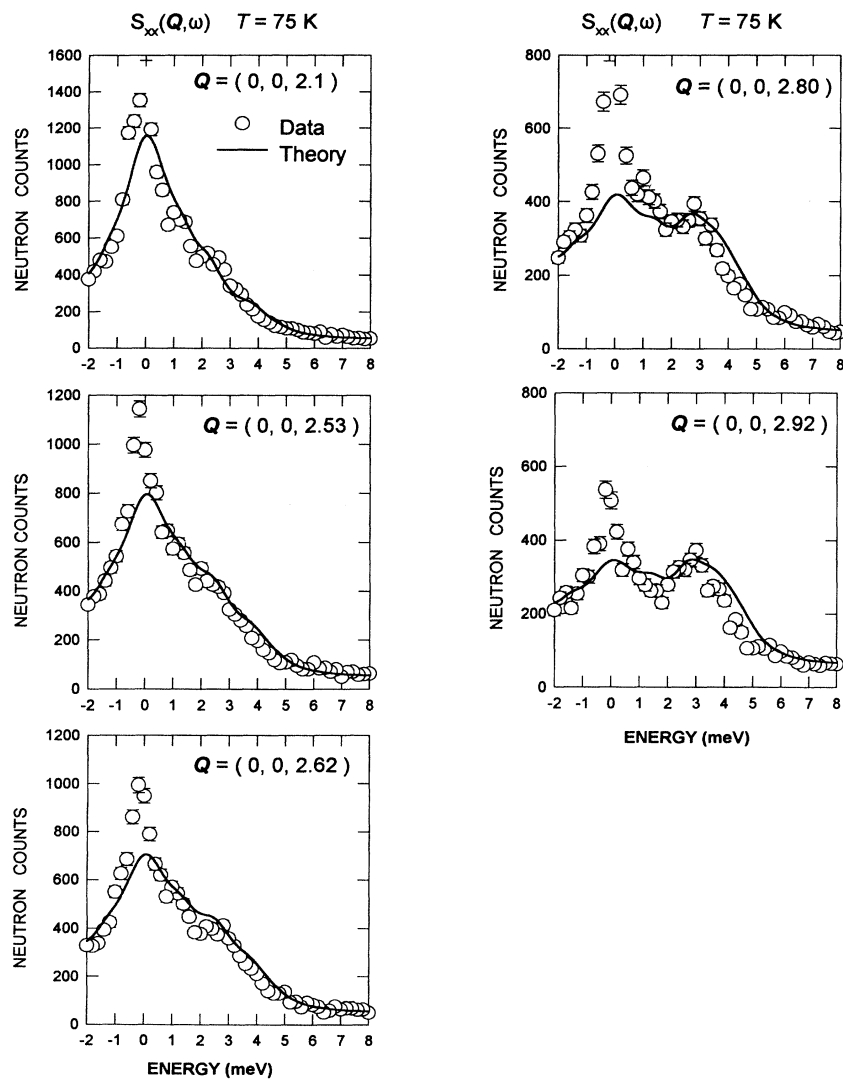

FIG. 3. Calculated and measured intensities for the transverse neutron-scattering function of erbium at 75 K.

atom is located at a node or at a crest of the CAM wave. Obviously for most atoms the transition to the first excited state represents an excitation energy of about 3–4 meV.

The results obtained for the transverse scattering at 75 K are shown in Fig. 3. Compared to the results for 60 K, the structure at finite energies for the smaller Q has diminished considerably, leading, apparently, to a small increase in the intensity at $\hbar\omega=0$. However, the scattering at larger Q has not changed much. As seen for 60 K, the theory reproduces the experimental observations quite well at all Q for excitation energies above about 1.0 meV, but not the quasielastic scattering.

A comparison between theory and experiment for the temperature dependence of the scattering at

$Q=(0,0,2.92)$ is shown in Fig. 4. Again, the theory reproduces well the experimental results above 1.0 meV, except for $T > T_N$. Even well above T_N at $T=200$ K, the theory predicts a peak in the scattering at finite energy that is not observed, although the overall magnitude of the observed scattering is reproduced fairly well even for $\hbar\omega=0$. Above T_N the molecular field at each site is zero. Consequently, as can be seen from the energy levels shown in Fig. 2, the predicted peak at about 2 meV is due to an abundance of crystal-field transitions at about this energy, even between excited levels.

The results obtained for $Q\perp c$ at $T=60$ K are shown in Fig. 5. Here the lines are theoretical calculations which are proportional to $S_{xx}(\mathbf{Q},\omega)+S_{zz}(\mathbf{Q},\omega)$. The factor $(1-Q_{zz}^2/Q^2)$ for $S_{zz}(\mathbf{Q},\omega)$ in Eq. (6) has been omitted in
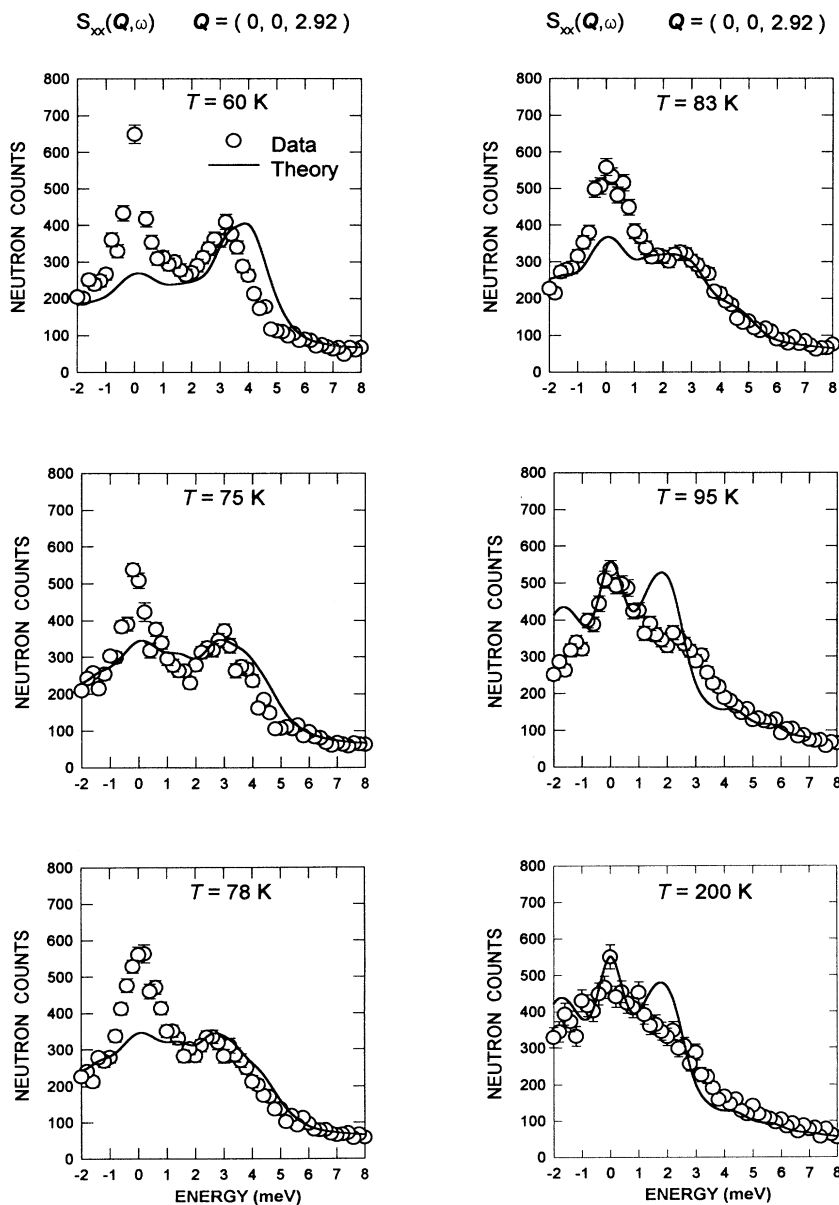

FIG. 4. Calculated and measured intensities for the transverse neutron-scattering function of erbium at $\mathbf{Q}=(0,0,2.92)$ as a function of temperature.

these calculations. It varies only slightly, from 1.0 to 0.92, in the range of Q shown in Fig. 5. The major part of the signal at $\hbar\omega=0$ is from $S_{zz}(\mathbf{Q},\omega)$, while above an energy of 1.0 meV the major part of the signal comes from $S_{xx}(\mathbf{Q},\omega)$. There is rather good overall agreement between the theory and experiment. It is interesting that the theory overestimates $S_{zz}(\mathbf{Q},\omega)$ at $\hbar\omega=0$, while, as seen in Fig. 1, it tends to underestimate $S_{xx}(\mathbf{Q},\omega)$.

The temperature dependence of $S_{xx}(\mathbf{Q},\omega)+S_{zz}(\mathbf{Q},\omega)$ at $(1,1,0.92)$ is shown in Fig. 6. There is a large increase of the calculated $S_{zz}(\mathbf{Q},\omega)$ for $T=75$ K which is not seen in the data. This result of the theory is not understood at this time. As seen also for $S_{xx}(\mathbf{Q},\omega)$ in Fig. 4, there is more structure at finite energy in the calculated scattering function at $T=200$ K than is observed. The calculat-

ed peak near 2 meV is from $S_{xx}(\mathbf{Q},\omega)$, and that at about 5 meV is from $S_{zz}(\mathbf{Q},\omega)$. We have found no peaks in the calculations which can explain our earlier observations[4] of an excitation with a linear dispersion relation near $(1,1,\tau_0)$ in the 60–85 K temperature range. It is possible that those results represent the observation of the phonon dispersion relation through the magnetovibrational scattering cross section.

The sensitivity of the theoretical results to the values of the model parameters has been examined by carrying out calculations for different crystal-field parameters but with the same exchange constants. Several different sets of crystal-field parameters, which have been deduced from different types of experimental measurements, have been reported for erbium.[3,10,12] The sets we have used are
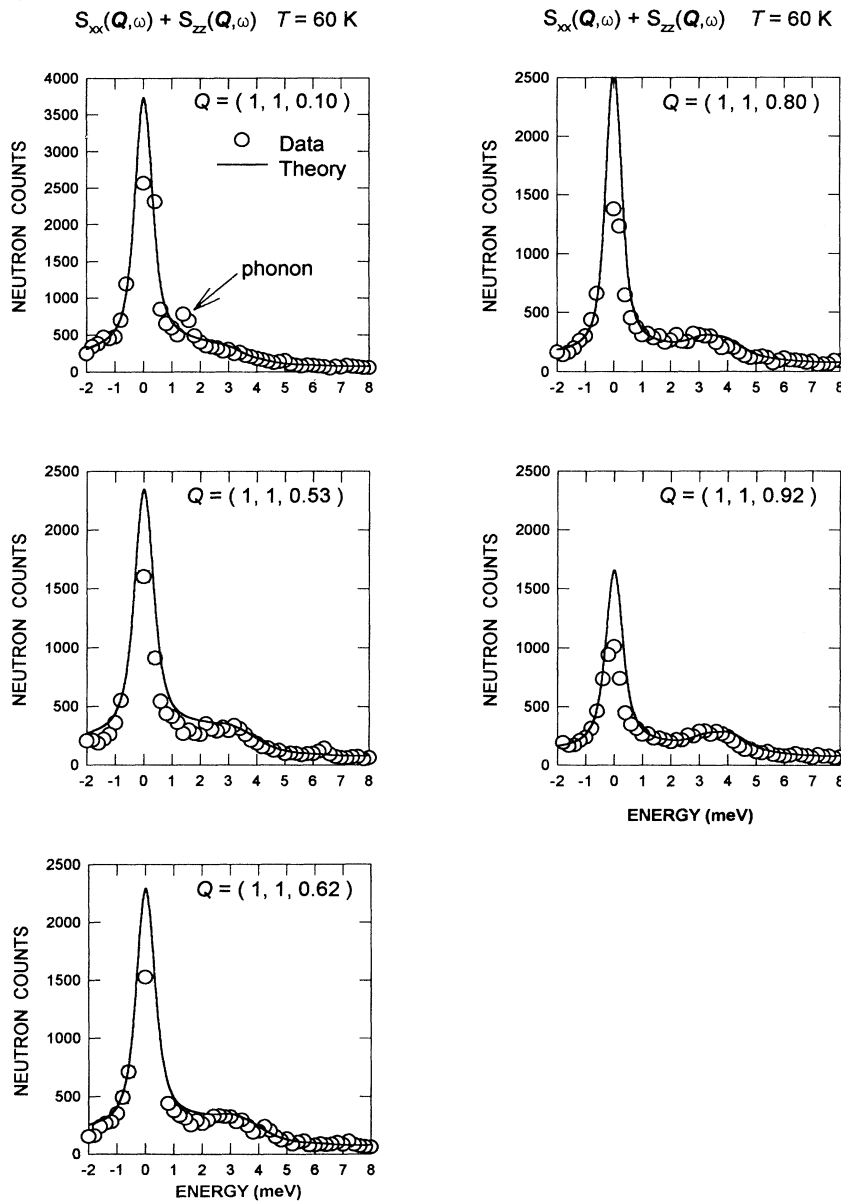

FIG. 5. Calculated and measured intensities for the sum of the transverse and longitudinal neutron-scattering function of erbium at 60 K.

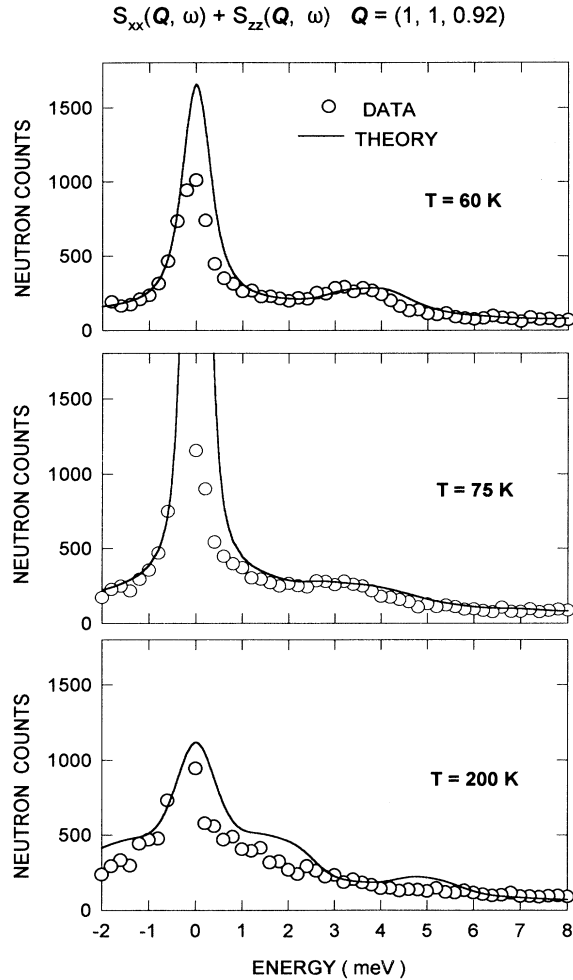$S_{xx}(\mathbf{Q}, \omega) + S_{zz}(\mathbf{Q}, \omega) \quad \mathbf{Q} = (1, 1, 0.92)$

FIG. 6. Calculated and measured intensities for the sum of the transverse and longitudinal neutron-scattering function of erbium at $\mathbf{Q}=(1,1,0.92)$ as a function of temperature.

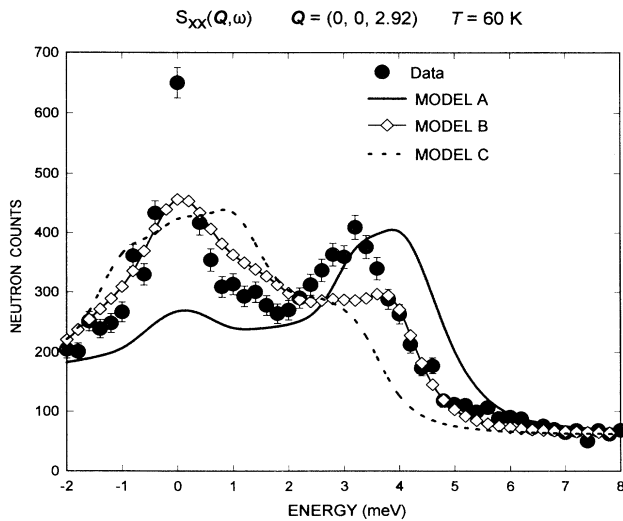$S_{xx}(\mathbf{Q},\omega) \quad \mathbf{Q} = (0, 0, 2.92) \quad T = 60\ \text{K}$

FIG. 7. Comparison of the measured intensity for the transverse scattering function of erbium at $\mathbf{Q}=(0,0,2.92)$ and $T=60$ K with the three models described in the text.

given in Table II. The $S_{xx}(\mathbf{Q},\omega)$ calculated with these parameters; models A, B, and C, are compared to the data for $\mathbf{Q}=(0,0,2.92)$ in Fig. 7. Model A is the one we have been comparing to the measurements in all the discussions above. It provides a rather good overall description of the experimental results, especially at finite energy, whereas model B gives a somewhat better description of the scattering near $\hbar\omega=0$ for large $\mathbf{Q}$. Model C does not reproduce very well any of the important features of the data. It is important to note that even with the same exchange parameters, the different sets of crystal-field parameters lead to slightly different theoretical T_N. As mentioned earlier, the comparisons between the data and theory are for the same T/T_N.

V. CONCLUSIONS

The magnetic excitations propagating along the c axis in the longitudinally modulated phase of erbium have been measured as a function of temperature by neutron inelastic scattering. The results for $T < T_N$ are in reasonable agreement with calculations based on the RPA theory reported by McEwen, Steigenberger, and Jensen[7] and parameters for the exchange and crystal-field interactions that have been published previously. However, not all sets of previously published crystal-field parameters leads to a satisfactory description of the data, at least not if the exchange interactions determined by Lindgård are used. We have not carried out calculations with any other sets of exchange parameters. The two significant shortcomings of the theory are (1) the failure to describe the quasielastic intensity for both the transverse and longitudinal scattering below T_N and (2) the prediction of structure at finite energy above T_N, which is not observed.

It appears that the RPA theory contains the important physics for understanding the neutron scattering by erbium in the CAM phase. In particular, the inclusion of the crystal-field interaction on an equal footing with the exchange interaction for determining the molecular-field Hamiltonian seems to be essential. Judging from the sensitivity of the calculated scattering function to the particular values of the crystal-field parameters, it is not surprising that the analytical treatments based on linear spin-wave theory, with only a single parameter to describe the magnetic anisotropy, do not work well for erbium.

[1]M. Habenschuss, C. Stassis, S. K. Sinha, H. W. Deckman, and F. H. Spedding, Phys. Rev. B **10**, 1020 (1974).

[2]H. Lin, M. F. Collins, T. M. Holden, and W. Wei, Phys. Rev. B **45**, 12 873 (1992).

[3]R. A. Cowley and J. Jensen, J. Phys. Condens. Matter **4**, 9673 (1992).

[4]R. M. Nicklow and N. Wakabayashi, Phys. Rev. B **26**, 3994 (1982).

[5]S. W. Lovesey, J. Phys. C. **21**, 2805 (1988); **21**, 4967 (1988).

[6]C. J. Lantwin, Z. Phys. B **79**, 47 (1990).

[7]K. A. McEwen, U. Steigenberger, and J. Jensen, Phys. Rev. B **43**, 3298 (1991).

[8]P. Lindgård, Phys. Rev. B **17**, 2348 (1978).

[9]R. M. Nicklow, N. Wakabayashi, M. K. Wilkinson, and R. E. Reed, Phys. Rev. Lett. **27**, 334 (1971).

[10]J. Høg and P. Touborg, Phys. Rev. B **11**, 520 (1975).

[11]J. W. Cable, R. M. Nicklow, and N. Wakabayashi, Phys. Rev. B **32**, 1710 (1985).

[12]J. Jensen and A. R. Mackintosh, *Rare Earth Magnetism. Structures and Excitations* (Oxford University Press, Oxford, 1992).